ACS APPLIED MATERIALS & INTERFACES

Forum Article

www.acsami.org

# Sequential Thiol Click Reactions: Formation of Ternary Thiourethane/Thiol–Ene Networks with Enhanced Thermal and Mechanical Properties

Olivia D. McNair, Davis P. Brent, Bradley J. Sparks, Derek L. Patton, and Daniel A. Savin*

School of Polymers and High Performance Materials, University of Southern Mississippi, 118 College Drive #5050, Hattiesburg, Mississippi 39406, United States

Supporting Information

**ABSTRACT:** We report the physical properties of thiol–ene networks modified with thiourethane or urethane linkages, either along the main chain or as a branched component in the network, respectively. Because of the robust and orthogonal nature of thiol-isocyanate and thiol–ene reactions, these networks can be formed in a two-step, one-pot synthesis. Resultant networks were characterized using dynamic mechanical analysis, mechanical testing and other complementary techniques. It was found that incorporating (thio)-urethanes into the networks increased $T_g$, but also increased strain at break and toughness while decreasing cross-link density. The changes in physical properties are discussed in terms of a proposed dual network morphology. These facile modifications to thiol–ene networks demonstrate how molecular-level, nanoscale changes can have a profound influence on the macroscale properties through hierarchical development of network morphology.

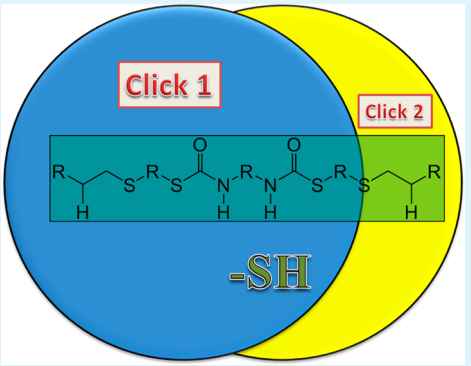


**KEYWORDS:** *thiol–ene, thiol-isocyanate, click chemistry, glass transition temperature, dual network*

## INTRODUCTION

The copolymerization of multifunctional thiol and vinyl monomers by ultraviolet light has been accomplished since the 1970s for the creation of coatings with excellent scratch resistance and high optical clarity.[1,2] Until recently thiol–ene networks (TENs) have remained grossly understudied, but the need for materials from facile and environmentally friendly syntheses has meant TENs are once again gaining prevalence into a wide variety of applications such as optics, biomedical, surface modification, composites, dental restoratives, and high-performance protective gear.[3−15] TENs are increasingly popular across a continuum of research areas because of their ease of fabrication, i.e., photopolymerizable click reactions under ambient conditions, and ideal network properties such as high energy damping and network uniformity. Specifically, thick thermoset TENs are being developed and investigated for their potentially high, nondestructive energy absorption capabilities, but networks in their native forms are not very useful because of low toughness.

Similar to other cross-linked networks, low strain translates to low toughness; therefore enhancing versatility of TENs means increasing toughness and temperature tunability. Though seemingly complex, the UV-initiated polymerizations of thiols with vinyl monomers are highly efficient and take place with or without catalyst under very mild conditions and in a predictable (i.e.: orthogonal) manner.[16−21] These and other specific properties of thiol–ene reactions prompted Sharpless and co-workers to classify the thiol–ene reaction into a category of "click reactions", setting the stage for a new way of thinking about organic synthesis in that reactions should be selected based on efficiency, simplicity, and selectivity.[3,16,20,22] As a result of this unique and efficient polymerization mechanism, TENs display exceptional physicomechanical properties such as low stress, uniform cross-link density, minimal chain-end presence, good adhesion to a variety of substrates, and high mechanical energy damping properties.[23] For example, a two-layer laminate thiol–ene disc constructed to be a few centimeters thick captured bullets shot from a 0.22 and 0.38 caliber without shattering.[23] This unique material behavior could be beneficial in many fields, especially the development of novel materials for personal protective equipment (PPE), as in the development of mouthguards to mitigate concussive events from impact.

One essential criterion for the success of thick thiol–ene thermosets is to produce novel materials capable of withstanding larger mechanical stresses. TENs synthesized from off-the-shelf monomers typically exhibit low glass-transition ($T_g$) temperatures, low strain at break, are brittle in nature, and have low toughness. For most PPE applications, robust materials must have high toughness while retaining the energy absorbing

**Special Issue:** Applications of Hierarchical Polymer Materials from Nano to Macro

**Received:** November 15, 2013
**Accepted:** February 14, 2014
**Published:** February 26, 2014

   dx.doi.org/10.1021/am405138e | *ACS Appl. Mater. Interfaces* 2014, 6, 6088–6097

capabilities at near-physiological temperatures. Researchers have attempted to modify physical properties of TENs by incorporating a third component such as an acrylate or isocyanate.[5,6,21,24−32] Acrylate networks are cured by UV polymerization, but are known to both homopolymerize and cross-polymerize with thiols in the presence of thiol and ene monomers. One drawback of this technique is that homopolymerization leads to phase separation of networks into acrylate rich and acrylate poor regions. Nonetheless, the network uniformity is increased compared to a native acrylate network, but the temperature range of energy dissipation is significantly broadened, compared with the native thiol−ene matrices, because of the increased network inhomogeneity. This results in a broad glass transition region.

Other approaches to improve toughness in TENs involve incorporation of urethane or thiourethane linkages. This generates a slight increase in network inhomogeneity, an increase in $T_g$, and an increase in toughness from intermolecular hydrogen bonding. Urethanes or thiourethanes have been incorporated into TENs in one of two ways: (1) synthesizing thiol or ene based monomers with reactive terminal ends followed by polymerization, or (2) utilizing one-pot synthetic techniques in which two catalysts are used, one for thiol/isocyanate reaction and a second for UV polymerization reaction.[25,28,29] The former method requires processing high viscosity monomers due to the hydrogen bonding between small molecules while the latter offers substantial synthetic and processing benefits. In 2010, Shin and co-workers synthesized ternary networks containing a difunctional thiol, trifunctional vinyl and trifunctional isocyanate monomers by sequential and simultaneous polymerization techniques yielding ternary TENs having $T_g$ values dependent on isocyanate content, as well as increased pendulum hardness, Young's modulus, peak stress, and elongation at break.[28]

Here we report the physical properties of TENs modified with thiourethane or urethane linkages, either along the main chain (i.e., as part of the primary network) or as a side-chain (i.e., branched) component in the network, respectively. In the former systems, modified TENs are produced whereby a dual-functional thiol first reacts with a diisocyanate, yielding linear oligomers containing thiourethane linkages. In the second step, the UV-initiated thiol−ene reaction is performed. Due to the robust and orthogonal nature of these reactions, it is able to be done in a two-step, one-pot process. For side-chain modified TENs, a bulky isocyanate is prereacted with a dual-functional ene containing a side-chain alcohol group. In contrast to previous thiol/ene/isocyanate studies, here the isocyanate reaction does not produce a covalent cross-link initially, but (thio)urethane linkages will facilitate hydrogen bonding in the network formed from the UV-initiated polymerization. An idealized network morphology is shown in Figure 1, where linear, hydrogen bonding thiourethane regions from the initial thiol-isocyanate reaction are interspersed in a covalent thiol−ene network. We compare the results of the modified TENs to both the unmodified networks and polyethylene-co-vinylacetate (EVA), a common material used in mouthguards, and other energy absorbing applications.

## EXPERIMENTAL SECTION

**Materials.** Isocyanates, enes, and catalysts were all purchased from Sigma Aldrich and used as received: isophorone diisocyanate (IPDI), 4,4′-methylenebis(cyclohexyl isocyanate) ($H_{12}$MDI), phenyl isocyanate (BZ), cyclohexyl isocyanate (CHX), and 1-napthyl isocyanate (NP) triallyl-1,3,5,-triazine-2,4,6(1H, 3H, 5H)-trione (TATAT), and pentaerythritol tetra(3-mercaptopropionate (PETMP), triethylamine (TEA) and dibutyl tin dilaurate (DBTDL). The photoinitiator, 2, 2-dimethoxy-2-phenylacetophenone (DMPA) was obtained from Ciba Specialty Chemicals. Thiol monomer, glycol di(3-mercaptopropionate) (GDMP), was generously donated by Bruno Bock Thio-Chemicals-S. Vinyl monomer Trimethylolpropane diallyl ether (TMPDE90) was donated by Perstorp and used as received.

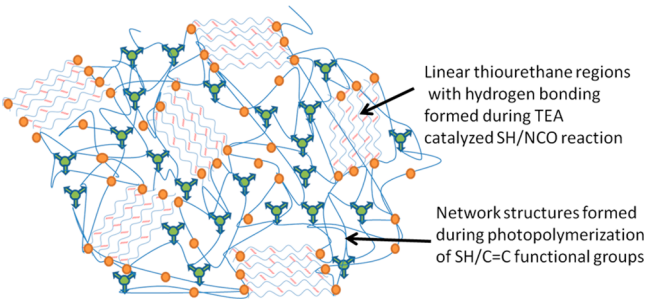


**Figure 1.** Proposed network structure of ternary thiol/ene/isocyanate networks.

**Synthesis and Sample Preparation for Main-Chain Thiourethanes.** Formulations of ternary thiol/ene/isocyanate networks were synthesized via a two-step, one-pot synthesis. In the first step, a tertiary amine catalyst (TEA) facilitates the thiol-isocyanate reaction and is followed by a traditional UV polymerization utilizing photocatalyst. The monomers and catalysts used are indicated in Figure 2. DMPA photoinitiator (1 wt % total formulation) was premixed and dissolved with GDMP by heating to 35 °C under sonication. After cooling, mixtures were covered to prevent premature curing before the vinyl curative TATAT was added. The isocyanate component (IPDI or $H_{12}$MDI) was then added with vigorous mechanical mixing. The isocyanate content was varied from 0 to 50 mol % such that the total (ene + isocyanate) content was stoichiometrically balanced with the total thiol. The composition range of the added isocyanate was chosen to minimize formation of inhomogeneities or gel formation from thiourethane-rich domains. In the final step, TEA (1 μL) was added, followed by rapid mechanical stirring. In unmodified systems with only thiol and ene components, TEA catalyst was eliminated.

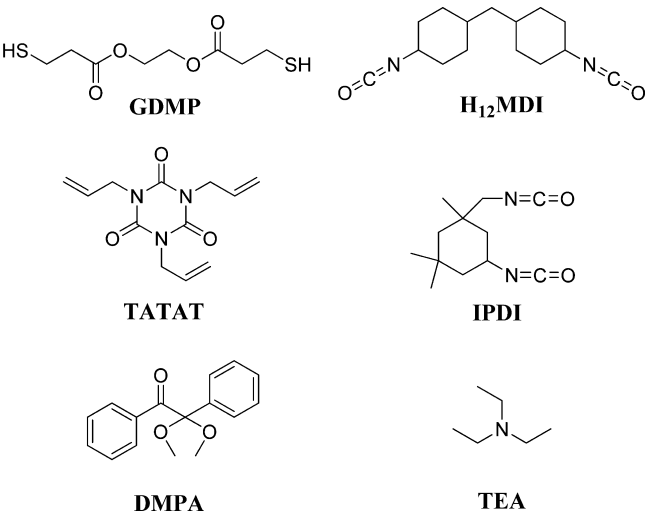


**Figure 2.** Momomers, isocyanates, and catalysts used for the main-chain incorporation of thiourethane linkages into TENs.

Films were produced by adding small amounts of thiol/ene/isocyanate mixtures into a rectangular Teflon mold of 0.5 mm thickness. Dogbones and tensile bars were formed by pipetting the


dx.doi.org/10.1021/am405138e | ACS Appl. Mater. Interfaces 2014, 6, 6088−6097

mixture into preformed silicon molds with appropriate dimensions. Dogbone molds were in line with ASTM test D638M, whereas tensile bar molds measured ca. 5.0 mm × 0.5 mm (width × thickness). The resulting films and bars were allowed to rest in ambient conditions for 30 min before irradiating with a low-pressure mercury UV lamp (intensity 20 mW/cm$^2$) for 30 min. The 30 min pre-UV time was necessary to permit thiol isocyanate reactions reach full conversion prior to initiating the UV polymerization reaction. Following UV treatment, all samples were postcured in an oven for 48 h at 90 °C.

**Synthesis and Sample Preparation for Branched Urethane-Modified TENs.** Divinyl monomers with bulky, urethane side groups were synthesized by addition of monofunctional isocyanates to the pendent alcohol group of TMPDE90 (Figure 3). One wt% DBTDL

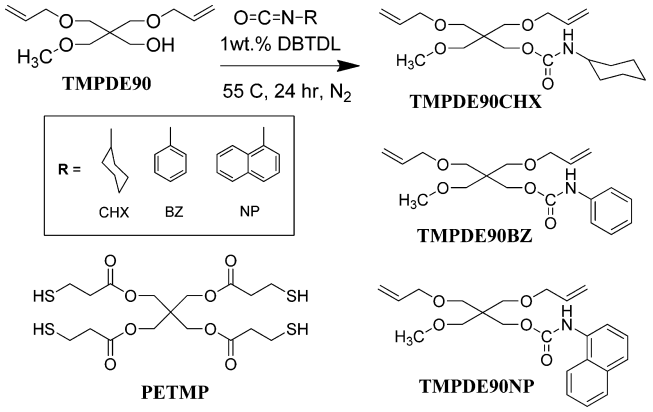


**Figure 3.** Momomers, isocyanates, and catalysts used for the incorporation of bulky branched urethane linkages into TENs.

was dissolved in TMPDE90 in a round-bottom flask over ice and purged with $N_2$ gas. BZ, CHX or NP was slowly added to the flask over a 30 min period from a $N_2$ filled holding chamber. Following complete isocyanate addition, the temperature was ramped to 55 °C over a one hour period where the mixture remained stirring overnight for a total of 24 h. Films were produced as indicated above with stoichiometrically balanced thiol/ene mixtures, with the exception that only the UV polymerization was performed.

**Kinetic Analysis Using FTIR and Real-Time FTIR.** Real-time FTIR (RT-FTIR) was performed on stochiometrically balanced mixtures of thiol to (alkene + isocyanate) in the case of main-chain thiourethanes. Kinetic analysis was investigated using mixtures of base monomers GDMP/TATAT along with 20 mol % of IPDI or $H_{12}$MDI and 1 wt % DMPA. A lower mol % NCO formulation was chosen due to the strong absorbance of isocyanate peaks. The peaks corresponding to thiol (2600 cm$^{-1}$) and alkene (2064 cm$^{-1}$) moieties were monitored with respect to time using a Nicolet 8700 FTIR spectrometer with a KBr beam splitter and a MCT/A detector along with a 320−500 nm filtered ultraviolet light source. The lamp, intensity ca. 20 mW/cm$^2$, was turned on at approximately 10 s, which marked the beginning of the UV reaction. Real-time data was collected for a total of 200 s at a 1/s scan rate of approximately 4 cm$^{-1}$. It should be noted that the alkene peak could not be monitored for benzene based mixtures (TMPDE90BZ/PETMP) due to the presence of strong alkene peaks associated with benzene; therefore the kinetic plot for that system only contains data for thiol conversion. Kinetic analysis was not performed for NP-based systems. From real-time measurements, we determined the conversion of thiol and ene functional groups with respect to time. From using FT-IR and RT-FTIR, the effects of isocyanate incorporation and isocyanate conversion, as well as UV network formation from the thiol-ene reaction, were precisely monitored.

**Thermal and Thermomechanical Testing.** Dynamic mechanical analysis (DMA) was performed on rectangular shaped samples that were prepared via UV-curing in silicon molds using a TA Q800 DMA (TA Instruments, New Castle, DE). Sample dimensions were kept consistent as length × width × thickness measured approximately (6 mm × 5 mm × 0.4 mm) for all samples. Beginning from a quench and one minute isothermal hold at −50 °C, samples were deformed in tensile mode to a 0.05% strain rate at 1 Hz frequency while being heated at 2 °C/min to a terminal temperature of 150 °C. Glass-transition temperature was recorded as the maximum temperature associated with the tan $\delta$ vs temperature curve, whereas glassy storage modulus ($E'_{glass}$) and rubbery storage modulus ($E'_{rubber}$) values were recorded from temperatures at $T_g$ − 40 K to $T_g$ + 40 K, respectively. Differential scanning calorimetry (DSC) was performed using a TA Q2000, TA Instruments, New Castle, DE. Approximately 7 mg samples were placed into standard aluminum pans and heated to 100 °C to erase thermal history, quenched to −40 °C, then reheated at 10 °C/min to 50 °C. The glass transition temperature was recorded from the second heating. Thermogravimetric analysis (TGA) was performed using TA Instruments TGA Q500. After equilibrating, ca. 8 mg samples in a standard platinum pan at 40 °C, they were heated at 10 °C/min to a terminal temperature of 800 °C. Sample mass loss was measured as a function of temperature, and polymer degradation temperature was determined from the peak values of the derivative weight (%/°C) versus temperature curve.

**Mechanical Testing.** Mechanical testing was performed using a Mechanical Testing System (MTS) Insight material testing machine equipped with a 1 kN load cell and preset to collect 10 data points per second. Dogbone (ASTM D638M) samples with cross-sectional dimensions 13.0 mm ± 0.5 mm and 3.5 mm ± 0.5 mm (width × thickness) were carefully centered in clamps, then deformed in tensile mode at a strain rate of 0.2 in/min. Young's modulus was calculated from the initial slope of the linear elastic region of the stress−strain curve. Peak load, peak stress, yield point, and strain at break were also determined concurrently during the tensile tests. Results presented are the average taken from 3−5 samples of the same formulation. Polymer density was determined by Archimedes' method. After allowing water to equilibrate to ambient conditions, moderately sized rectangular samples were weighed in air then reweighed while immersed in water. The difference between the two masses was then used to determine the density of polymer samples. To ensure accurate measurements, water bath temperature was measured occasionally between runs. Polymer density was calculated in g/cm$^3$ for four samples of each formulation, and values shown in the following discussion represents an average value along with standard deviations. Material response upon impact was measured using a Dynatup 9250 HV equipped with a 88 kN load cell. Thiol−ene and EVA discs measuring 2″ in diameter and 4 mm in thickness were impacted using a steel drop dart and impact energy of 4.4 J. The corresponding impact specifications utilized an impact velocity = 1.25 m/s, drop height =0.08 m, and drop mass = 5.6 kg. The samples were centered on top a hardened steel anvil to prevent flexion, and a pneumatic brake was applied automatically following impact to prevent a second incidence of impact. Atmospheric conditions at the time of testing were 23 °C and 42% relative humidity.

**Scanning Electron Microscopy.** Fracture surfaces from tensile tests were imaged using scanning electron microscopy (SEM). A small slice of the fracture surface perpendicular to force direction was removed and sputter-coated with high-purity gold using a standard technique. Samples were charged under argon gas and 25 mA for 3 min, resulting in a gold coating of approximately 10 nm. SEM images were taken using SEM Quanta FEI 200 at 100× magnification.

## RESULTS AND DISCUSSION

**Kinetics of Dual Cure Thiol−ene-Isocyanate Networks; Networks Containing Main-Chain Thiourethane Linkages.** In this study, we investigated thermal and mechanical properties of ternary thiol−ene-isocyanate networks to determine changes in material properties with respect to isocyanate structure, isocyanate content and network morphology. We investigated the reaction kinetics of the main-chain dual cure systems for each sample with respect to the thiol-

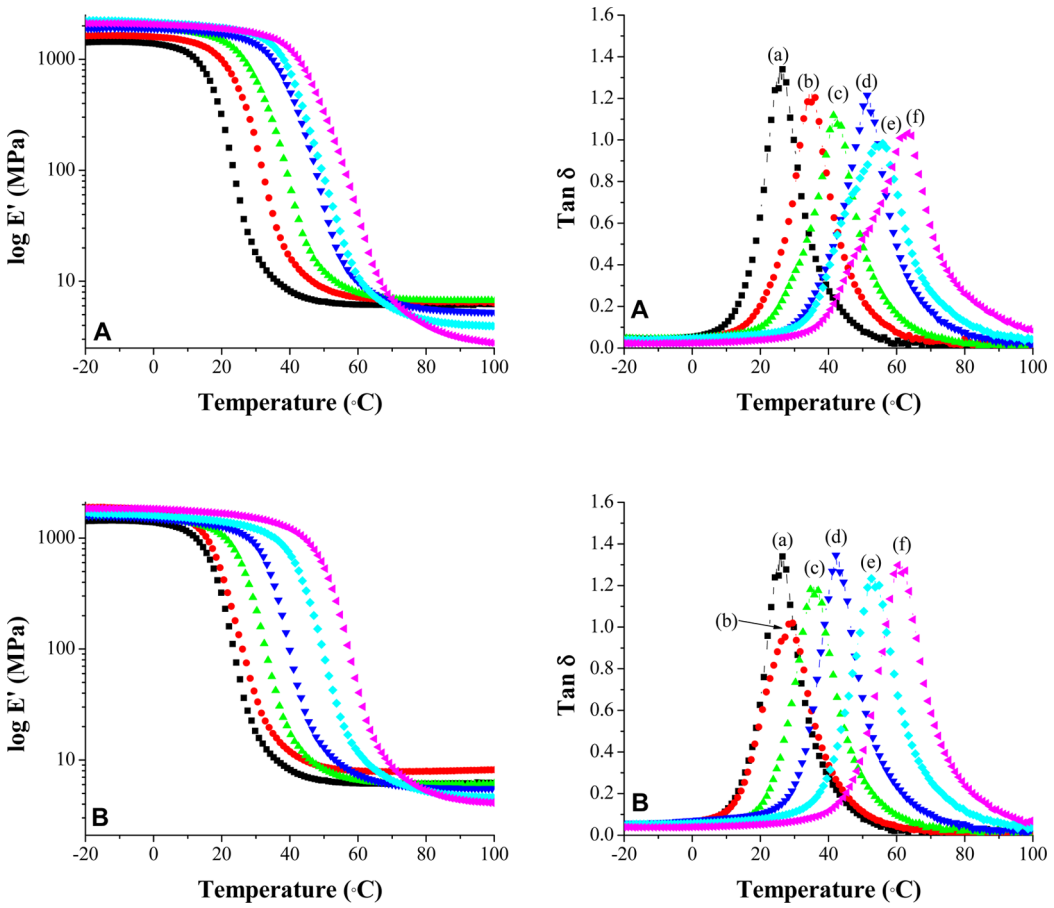


**Figure 4.** $E'$ (left) and tan $\delta$ (right) vs temperature from DMA measurements of ternary thiol/ene/isocyanate of (A) GDMP-TATAT-IPDI and (B) GDMP-TATAT-$H_{12}$MDI from −20 to 100 °C, heating at 5 °C/min. Isocyanate content was varied from 0 to 50 mol % in the following ratios: GDMP/TATAT/NCO 100/100/0 (black square), 100/90/10 (red circle), 100/80/20 (green triangle), 100/70/30 (blue triangle), 100/60/40 (aqua diamond), and 100/50/50 (magenta triangle).

isocyanate reaction (performed first) and the UV-initiated thiol−ene polymerization (performed second, in the same pot). Individual peaks for each thiol (≈ 2551 $cm^{-1}$) and isocyanate (2250 $cm^{-1}$) functional groups were observed using FTIR analysis before and after TEA catalyst addition (5 min reaction time). The initial thiol-isocyanate reaction was evident by the disappearance of the isocyanate peak at 2250 $cm^{-1}$ and appearance of a peak around 3350 $cm^{-1}$ (see Figure S1 in the Supporting Information). The broad peak at 3350 $cm^{-1}$ relates to the N−H stretch of the newly formed secondary amide structures that are associated or involved with hydrogen bonding. The second reaction involved the UV-initiated thiol−ene reaction between thiol-terminated, thiourethane-containing oligomers and any excess thiol with ene monomer. Here, the RT-FTIR was used whereby the peak intensity of thiol and ene peaks are measured with respect to time. Figure S2 in the Supporting Information confirms vinyl group conversion was greater than 95% for all systems thereby verifying thiol−ene photopolymerization indeed proceeded in the second step and not the first. The thiol conversion in this step was slightly lower than quantitative, potentially because of the self-polymerization of TATAT exasperated by the viscous thiourethane-containing oligomers. Nonetheless, this one-pot synthetic method is a facile way to produce ternary networks with dual network morphologies.

**Kinetics of Thiol−ene-Isocyanate Networks Containing Branched Urethane Substituents.** FTIR was first used to demonstrate successful incorporation of urethane-linked side-chains (see Figure S3 in the Supporting Information). Then, RT-FTIR was used to follow network formation using modified ene monomers. The kinetic profile for the systems containing novel alkene monomers with branched urethanes were similar to typical thiol−ene kinetic profiles. The RT-FTIR of a native matrix, PETMP-TMPDE90, was performed as a control system and demonstrated quantitative conversion for both thiol and alkene functional groups within a matter of seconds (see Figure S4 in the Supporting Information). The kinetic plot of PETMP-TMPDE90CHX was similar to the kinetic plot of the control (see Figure S5 in the Supporting Information). It can be inferred that the bulky cyclohexyl group has little effect on ene monomer reactivity. The benzene (BZ) based system was more difficult to observe with respect to reaction kinetics due to the presence of double bonds associated with the benzene ring. However, the kinetics of the thiol functional group was still able to be monitored. Assuming the thiol conversion mirrors alkene conversion, it is seen from Figure S6 (see the Supporting Information) that the overall conversion of thiol was lower, but still exceeds 90% after 60 s of irradiation.

**Physical Properties of Thiol−ene-Isocyanate Networks.** Discussion of the thermomechanical and mechanical properties of thiol−ene-isocyanate networks will be divided into two groups. First, the incorporation of thiourethanes along the main chain will be presented and discussed in terms of a


dx.doi.org/10.1021/am405138e | ACS Appl. Mater. Interfaces 2014, 6, 6088−6097

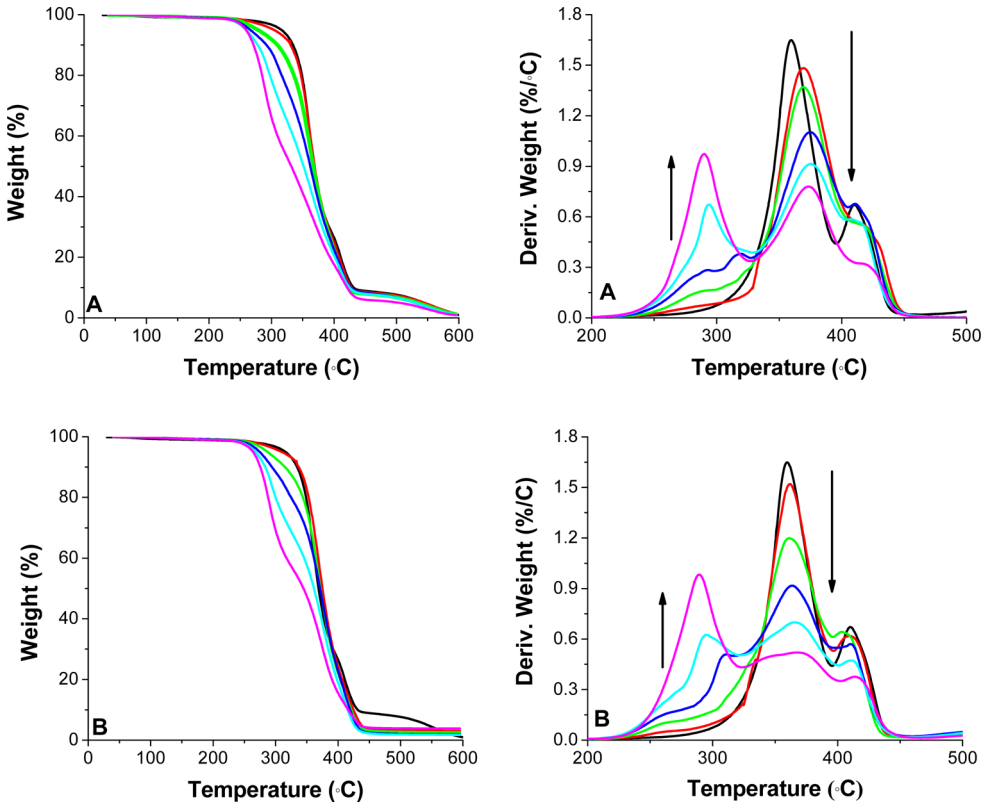


**Figure 5.** Thermogravimetric analysis of ternary TENs with 0−50 mol % isocyanate content, (A) GDMP-TATAT-IPDI and (B) GDMP-TATAT-$H_{12}$MDI. Left: Weight loss as a function of temperature. Right: Derivative weight loss as a function of temperature. Thiol:ene:isocyanate content 100/100/0 (black), 100/90/10 (red), 100/80/20 (blue), 100/70/30 (green), 100/60/40 (cyan), and 100/50/50 (magenta).

dual network morphology. Second, the TENs modified with branched urethanes will be discussed.

**Thermomechanical Properties of Main-Chain Thiourethane Containing Networks.** Films of ternary networks were subjected to small oscillatory tensile strains in order to resolve the storage modulus ($E'$), the loss modulus ($E''$) and tan $\delta$ (ratio of $E''/E'$). Figure 4 shows results from DMA, and three major trends emerge: (1) $E'$ increases in the glassy regime with increased NCO content, (2) the glassy plateau in modulus is extended with increased NCO content (i.e., $T_g$ increases), and (3) $E'$ in the rubbery plateau decreases with increasing NCO content. The first and second observations are likely due to the network structure of the isocyanate additive, as both IPDI and $H_{12}$MDI systems contain rigid monomer, and hydrogen bonding between thiourethane groups would increase the effective cross-link density. Because of this incorporation of rigid, hydrogen bonding components, the $T_g$ is also expected to increase. The last observation, that the E′ in the rubbery plateau regime decreases with increasing isocyanate content, can be explained by the decrease in cross-link density with increasing isocyanate content; this is a direct result from chain extension of the difunctional thiol monomer GDMP with the difunctional isocyanates in the first reaction. At higher temperatures, effects from hydrogen-bonding would be negligible; therefore systems with high NCO content would have lower effective cross-link densities and therefore exhibit low values of $E'$. It has been shown previously that addition of dual-functional (i.e., chain extending) components into TENs serves to increase cross-link density.[33]

The breadth of the tan $\delta$ versus temperature curve directly relates to network uniformity, and traditional TENs exhibit very narrow tan delta vs temperature curves as confirmation of high uniformity of the networks. Figure 4 shows a very slight broadening of the curves for both urethane systems as isocyanate content increases. Broadening of the curves indicates increased heterogeneity, which could be explained by the presence of a second, urethane-rich, domain in the network morphology. Prior studies of EVA and acrylate-functionalized TENs show considerable broadening of the tan $\delta$ in the glass transition region.[5,8,9,15] While this may be beneficial for applications requiring a wide range of operating temperatures, mouthguards and PPE require maximum energy dissipation in the vicinity of 37 °C. Thiol−ene networks here retain this high mechanical loss after modification.

As mentioned previously, the glass transition temperature shifts toward higher temperatures for all ternary systems as isocyanate content increases. The increase in $T_g$ is a result of a combination of structural effects along with hydrogen bonding. It is shown in Figure 4 that $T_g$ is increase by 35−37 °C up to 50 mol % incorporation of diisocyanate. Cyclic aliphatic groups are bulky and known to increase $T_g$ of many networks, and it is observed that $T_g$ increases with isocyanate content (i.e., bulky, hydrogen-bonding main-chain components arrest segmental motion). This is a significant observation because it is possible that hydrogen bonding is more effective in ternary TEN systems based on linear precursors which are reacted first, and this could allow for more efficient orientation of hydrogen within H-bonding regions. The complete results from DMA analysis are given in Table S1 (see the Supporting Information).

If difunctional thiols and difunctional isocyanates are utilized in sequential polymerizations, this would theoretically yield

linear thiol-isocyanate regions that would be embedded within a thiol−ene matrix upon completion of the thiol−ene reaction step. As such, we investigated the thermal degradation of these ternary networks for formulations with up to 50 mol % isocyanate content (Figure 5). It was found that in general the onset of polymer degradation decreased with increasing isocyanate content. A plot of the derivative weight loss with respect to temperature shows an increase in an unresolved feature that has a lower degradation temperature compared with the main degradation. This finding is in good agreement with the hypothesized presence of two domains, one linear system composed of linear thiol-isocyante regions and a second composed of the network system. In fact, the curve attributed to the degradation of unmodified network (around 340 °C) decreases in intensity as the second feature at lower degradation temperature appears. This second feature does not appear until the isocyanate content is around 20 mol %, thus we attribute this mass loss to the decomposition of isocyanate-containing linear regions within the network. These findings are consistent with a two-phase network morphology.

**Mechanical Testing of Main-Chain Thiourethane Containing Networks.** Stress−strain relationships of TENs containing cyclic aliphatic diisocyanates were measured using ASTM D638 M standard dogbone samples and standard Instron tensile test methods. Representative stress/strain curves are shown in Figure 6, and the averaged results are presented in Table S1 in the Supporting Information. The neat GDMP/TATAT matrix had a Young's modulus of 9.7 MPa and a maximum strain at break of 25%, which are typical for cross-linked TEN systems with $T_g$ values close to ambient temperature. The urethane-modified networks showed significant increases in the Young's modulus, increasing from 9.7 MPa (native matrix) to 600 and 1320 MPa for formulations containing 50 mol % isocyanate (IPDI and $H_{12}$MDI, respectively) content. The increase in modulus can be contributed to a combination of both hydrogen-bonding and increased $T_g$. Polymer density measurements were also in good agreement with the proposed dual network structure and initial chain extension reaction. Figure S7 shows that polymer density decreases nearly linearly from 1.35 to 1.26 g/cm$^3$ for IPDI and $H_{12}$MDI samples with increasing NCO content. This suggests that although there exists hydrogen bonding in the network below $T_g$, the bulkiness of the isocyanate linker dominates in terms of the bulk density. Such a decrease in polymer network density is also evident by observed differences in the aforementioned $E'$ rubber plateau values.

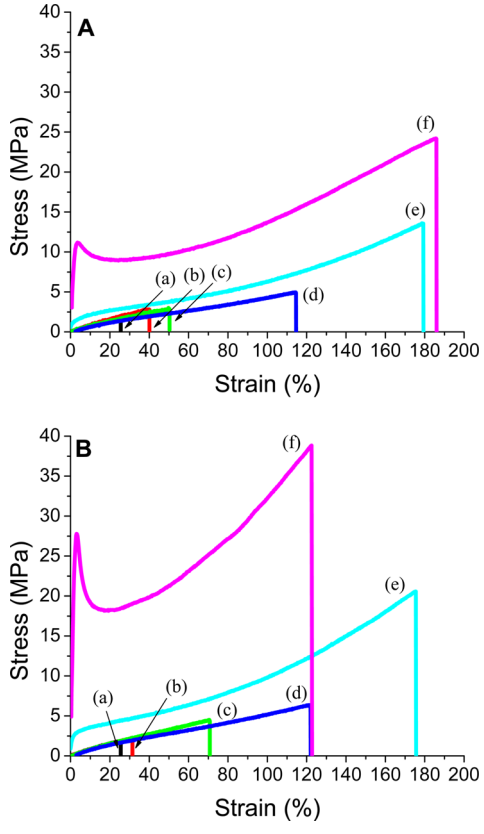


**Figure 6.** MTS data for SH/ENE/NCO formulations containing (A) IPDI (top) and (B) $H_{12}$MDI (bottom) as follows: (a) 00/100/0, (b) 100/90/10, (c) 100/80/20, (d) 100/70/30, (e) 100/60/40, and (f) 100/50/50. Mechanical testing was performed using a 10 kN load cell while samples were deformed at 0.2 in/min.

One of the most desired combinations of polymer mechanical properties is high modulus with high strain at break. In general, these properties of mutually exclusive, i.e., there is a trade-off between modulus and elongation. In contrast, the systems synthesized for this investigation demonstrated improvement in both modulus and strain at break. TENs have lower moduli due to the presence of flexible thioether groups, but also low elongation due to network homogeneity. When bulky isocyanate monomers are incorporated, forming a linear amorphous region, the effects of hydrogen bonding and higher $T_g$ enhance modulus and strain at break, making it possible to achieve both simultaneously. It is important to note that although modified TENs show a 10-fold increase in strain at break compared with the native network, they still lag behind EVA, which has a reported strain at break of 1400%.[34]

As previously mentioned, the first reaction in the sequential process is a chain extension reaction which yields linear oligomers with thiol end groups and thiourethane linkages. Figure 7 shows that the stain at break and engineering toughness is increased for TENs as isocyanate incorporation increases for both IPDI and $H_{12}$MDI networks. Strain at break increased for formulations containing up to 40 mol % isocyanate content followed by a slight decrease in strain at break for 50 mol % isocyanate content. This crossover behavior was observed in previous systems and is believed to result from a delicate balance between structural effects and hydrogen bonding.[28] For example, the increase in strain at break, along with the development of yield point for systems containing 50 mol % isocyanate content, is evidence that there is an increase in the size of linear domains within the ternary networks resulting from the thiol-isocyanate reaction. These linear regions will exhibit extensive hydrogen bonding, resulting in a much higher Young's modulus, but then yield upon disruption of hydrogen bonds. In addition, the slight decrease in strain at break is likely the result of thiourethane-rich domains at that high isocyanate content. This would act in a way similar to a heterogeneous crystalline domain in a traditional thermoset, which would reduce the effective hydrogen bonding between elastically effective chains, although this has not been determined conclusively in this study. As mentioned, the yielding comes from initial breakdown of hydrogen bonding in thiourethane domains that do not subsequently engage in hydrogen bonding while under stress, and the increased strain


dx.doi.org/10.1021/am405138e | ACS Appl. Mater. Interfaces 2014, 6, 6088−6097

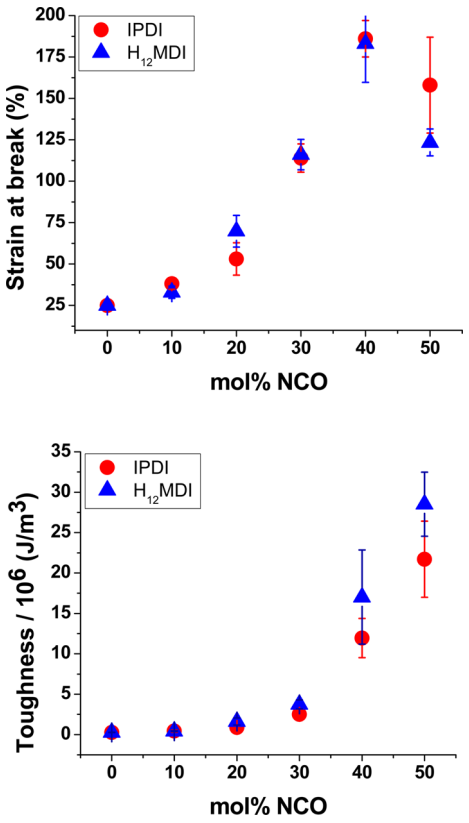


**Figure 7.** (Top) Toughness, calculated from integral beneath stress–strain curves from MTS tensile experiments. (Bottom) Strain at break for ternary thiol–ene isocyanate networks containing between 0 and 50 mol % isocyanate content: IPDI (red circles), and $H_{12}$MDI (blue triangles).

at break results from an increase in molecular weight between cross-links.

The incorporation of isocyanates along the main chain of TENs has been shown to increase $T_g$ while simultaneously increasing strain at break and toughness. As mentioned, this is due to a dual network morphology containing hydrogen bonded thiourethane linear regions (from the initial thiol-isocyanate reaction) embedded within a photopolymerized thiol–ene permanent network. The next section of the discussion will focus on the incorporation of branched urethanes in a permanent TEN. In these networks, the isocyanate content will not be varied, rather each ene monomer will contain the branched substituent. Similar to above, we retain hydrogen-bonding capabilities where the urethane linkages are close to a cyclic component.

**Thermomechanical Properties of Branched Urethane Containing Networks.** Thermal properties of network films were measured using DSC (see Figure S7 in the Supporting Information). The $T_g$ was measured for the control network PETMP-TMPDE90 as well as the networks containing novel bulky alkene monomers to be −21, 7, 10, and 12 °C for PETMP-TMPDE90, PETMP-TMPDE90CHX, PETMP-TMPDE90BZ, and PETMP-TMPDE90NP, respectively (see Figure S7 in the Supporting Information). The glass transition temperatures of the networks from bulky-based alkene monomers were considerably higher than the control network. The presence of bulky side groups along the backbone of the polymer chain is known to shift glass transition temperatures to higher values. Additionally, hydrogen bonding between pendant urethane groups is likely to cause the same effect such that the overall glass-transition temperature is higher.

The viscoelastic properties of the network systems were measured using DMA. Figure 8 shows the storage modulus

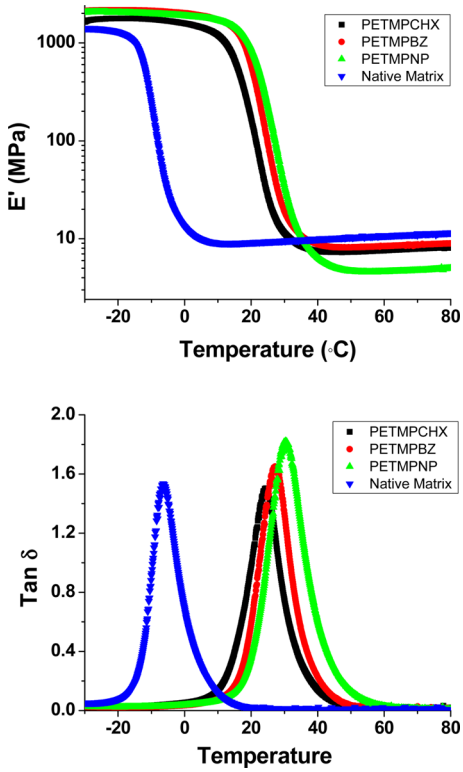


**Figure 8.** DMA measurements for TENs containing novel alkene monomers modified with bulky isocyanates. (Top) Storage modulus $E'$ vs temperature. (Bottom) Tan $\delta$ vs temperature. The legend indicates the modified ene used for the network in stoichiometric equivalence with thiol (i.e., CHX = cyclohexyl, BZ = benzyl, and NP = naphthyl).

($E'$) with respect to temperature for each of the network systems. It is observed that both the glassy modulus and $T_g$ increase with the incorporation of branched isocyanates, similar to what was observed in the main-chain isocyanate-functionalized networks above and linear polymers containing branches. As mentioned above, the breadth in the tan $\delta$ vs temperature curve directly relates to network uniformity. In contrast to incorporation of main-chain isocyanates above, in the case of branched modified TENs the narrow glass transition region is retained (Figure 8, Bottom). In fact, the width in the transition region for the modified networks is nearly identical to the native network. This demonstrates high network homogeneity, and it appears here that this is not compromised from a new monomer structure. Above $T_g$, the storage modulus decreases approximately 2 orders of magnitude and reaches a second rubbery plateau at higher temperatures. The modulus of this plateau is directly proportional to cross-link density. The unmodified network demonstrates the highest rubbery plateau, corresponding to the most tightly cross-linked system. Incorporation of branched substituents serves to increase the molecular weight between cross-links, thereby reducing cross-link density. It is observed that the CHX and BZ systems have roughly the same rubbery modulus, consistent with the similar


dx.doi.org/10.1021/am405138e | ACS Appl. Mater. Interfaces 2014, 6, 6088–6097

molecular weights. In contrast, the larger NP substituent shows a lower rubbery modulus.

**Mechanical Testing of Branched Urethane Containing Networks.** The tensile properties for side-chain modified TENs were determined using MTS in order to study the effects of bulky side groups and hydrogen bonding. The tensile modulus, peak load and strain at break were determined for stoicheometrically balanced networks (excluding PETMP-TMPDE90NP, as this sample was cost-prohibitive for replicated measurements); these results are tabulated in Table S3 (see the Supporting Information). It is clear that the unmodified network shows poor strain at break. This is common for TENs with high network homogeneity, even if the $T_g$ of the network is low. In contrast, there was a considerable increase in the strain at break for the modified systems PETMP-TMPDE90CHX and PETMP-TMPDE90BZ (Figure 9). Strain at break for these systems was 5−6 times higher, on average, compared to the native matrix material. This enhancement is likely due to side chain interactions and hydrogen bonding; at room temperature hydrogen bonds would play a considerable role in toughening even though the material is very near $T_g$. In contrast to main-chain isocyanate incorporation above, the increase in strain at break for branched isocyanates was compromised by lower modulus values. The nature of this observation lies in the fact that monomers with bulky groups led to network systems with a lower cross-link density, and the material is not in the glassy state at testing conditions. SEM imaging of fracture surface revealed considerable differences between the systems. Figure S9 shows the brittle nature of the failure associated with the unmodified network materials. This corresponds to the higher modulus and higher brittleness. The two systems modified with branched isocyanates demonstrate a much smoother fracture surface, consistent with more ductile failure, lower modulus and higher elongation.

**Impact Properties of Branched Thiol−ene Networks.** Viscoelastic properties from DMA showed that side-chain modified networks have high loss moduli near ambient temperatures, therefore we measured the impact properties via a linear drop tower testing system. The important parameters in this experiment are peak load (the highest force realized upon the impact event), time to peak load, overall time of an impact event, and curve shape. The peak load corresponds to the force that is transferred through the material. A lower peak load corresponds to increased energy dissipation by the material.[35] Impulse curves are shown in Figure 10. All tested thiol−ene materials had lower peak load compared withEVA. The peak load values on average were 7820, 6690, 7000, and 5680 N for EVA, PETMP-TMPDE90CHX, PETMP-TMPDE90BZ and PETMP-TMPDE90 respectively. Figure 10 also shows that time to peak force may be slightly lower for thiol−ene systems modified with branched substituents. These materials have higher glass transition temperatures and would likely have less deformation upon initial impact because the materials are stiffer at the tested temperatures.[35] The unmodified PETMP-TMPDE90 network however shows a longer time response and a characteristic trapezoidal shaped curve. The longer time response is a result of the lower glass transition temperature associated with the network and more deformation during the impact event. Although all TENs had lower peak force than EVA, it is clear that the higher $T_g$ in the branched modified networks failed to reduce peak force through energy dissipation in the network.

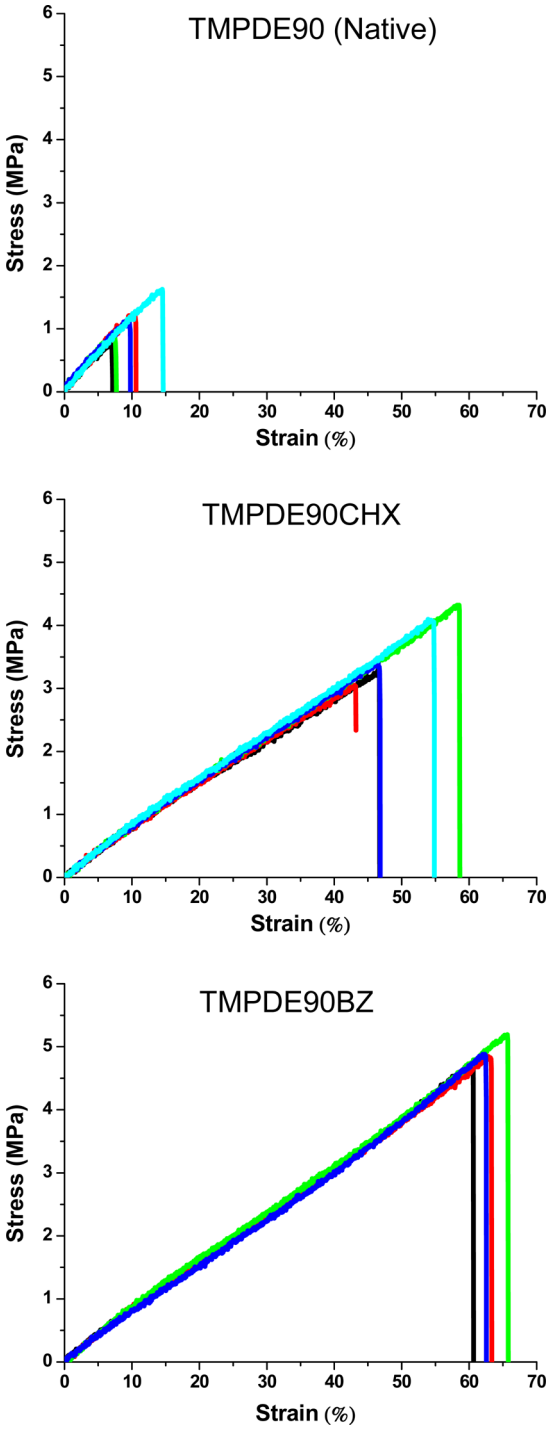


**Figure 9.** MTS tensile curves of novel TENs from branched alkene monomers.

## CONCLUSIONS

We have investigated the physical properties of thiol−ene networks modified with thiourethane or urethane linkages, either along the main chain or as a branched component in the network, respectively. Due to the robust and orthogonal nature of thiol-isocyanate and thiol−ene reactions, these networks can be formed in a two-step, one-pot synthesis. In the former case, ternary thiol−ene isocyanate networks were synthesized using a


dx.doi.org/10.1021/am405138e | ACS Appl. Mater. Interfaces 2014, 6, 6088−6097

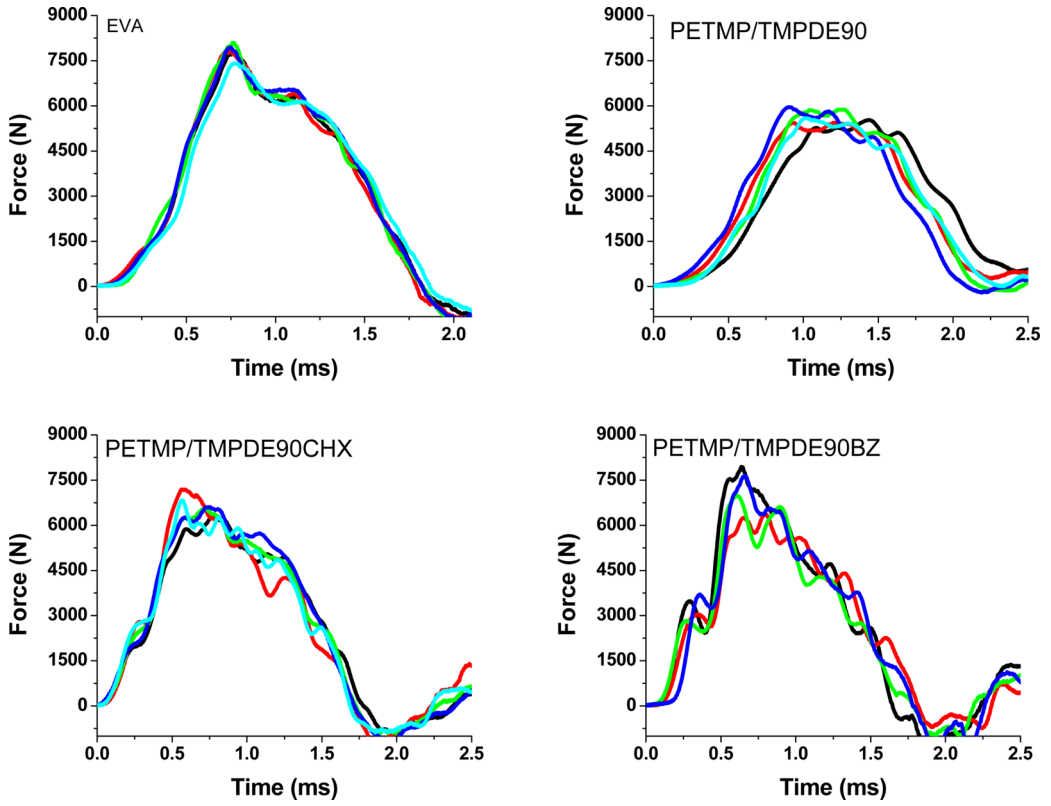


**Figure 10.** Impact curves for EVA and TENs containing bulky alkene monomers. Each curve represents and individual impact, and five impacts were taken for independent samples of each formulation.

one-pot method, and kinetic analysis demonstrated that the initial thiol-isocyanate reaction proceeds independently from the second thiol−ene photopolymerization. DMA results show that increasing the mol % of cyclic aliphatic isocyanates increases the glassy modulus and $T_g$, but lowers the rubbery modulus due to a decrease in cross-link density. Tensile properties of ternary networks demonstrate a combination of increased Young's modulus, strain at break and engineering toughness. For branched urethanes, it was demonstrated that $T_g$ is increased for modified networks compared to the native systems. Mechanical properties were also enhanced with respect to strain at break; however, this was compromised by lower moduli. The impact properties were measured using a drop test system with an energy relevant for a mouthguard material. The results demonstrate that TENs outperform EVA mouthguard material with respect to peak load values, however time to peak load was comparable. The viscoelastic properties and thermal response of networks containing linear (thio)-urethanes are manipulated through simple sequential chemistries yielding dual network morphologies. These facile modifications to thiol−ene networks demonstrate how molecular-level, nanoscale changes can have a profound influence on the macroscale properties through hierarchical development of network morphology.

## ■ ASSOCIATED CONTENT

### Supporting Information

FTIR and RT-FTIR spectra, SEM, density, and additional DSC data, as well as tabulation of thermomechanical data. This material is available free of charge via the Internet at http://pubs.acs.org.

## ■ AUTHOR INFORMATION

### Corresponding Author

*E-mail: daniel.savin@usm.edu. Phone: 601-266-5395. Fax: 601-266-5504.

### Notes

The authors declare no competing financial interest.

## ■ ACKNOWLEDGMENTS

The authors gratefully acknowledge funding from the Office of Naval Research (Award N00014-07-1-1057). ODM and BJS were supported by the U.S. Dept. of Education GAANN Fellowship Program (Award P200A090066). We thank Prof. Jeffrey Wiggins for use of his DSC and Emily Hoff (Patton Group) for useful discussion. We acknowledge Bruno Bock and Perstorp for donating commercial monomers used in this study.

## ■ REFERENCES

(1) Chen, Z.; Chisholm, B. J.; Patani, R.; Wu, J. F.; Fernando, S.; Jogodzinski, K.; Webster, D. C. Soy-based UV-curable thiol-ene coatings. *J. Coat. Technol.* **2010**, 1−11.

(2) Midgley, T., Jr; Henne, A. L.; Shepard, A. F. Natural and Synthetic Rubber. XII. Reversible Vulcanization, By Organo-Metallic Derivatives. *J. Am. Chem. Soc.* **1934**, *56* (5), 1156−1157.

(3) Hoyle, C. E.; Bowman, C. N. Thiol-ene Click Chemistry. *Angew. Chem., Int. Ed.* **2010**, *49* (9), 1540−1573.

(4) Hoyle, C. E.; Gould, T.; Piland, S.; Wei, H.; Phillips, B.; Nazarenko, S.; Askim, F.; Cole, M. Photocurable materials for mouthguards. *Radtech Rep.* **2006**, 12−17.

(5) Senyurt, A. F.; Wei, H. Y.; Hoyle, C. E.; Piland, S. G.; Gould, T. E. Ternary Thiol-ene/Acrylate Photopolymers: Effect of Acrylate Structure on Mechanical Properties. *Macromolecules* **2007**, *40* (14), 4901−4909.

(6) Wei, H. Y.; Senyurt, A. F.; Jonsson, S.; Hoyle, C. E. Photopolymerization of Ternary Thiol-ene/Acrylate Systems: Film and Network Properties. *J. Polym. Sci., Part. A: Polym. Chem.* **2007**, *45* (5), 822−829.
(7) Campos, L. M.; Meinel, I.; Guino, R. G.; Schierhorn, M.; Gupta, N.; Stucky, G. D.; Hawker, C. J. Highly Versatile and Robust Materials for Soft Imprint Lithography Based on Thiol-ene Click Chemistry. *Adv. Mater.* **2008**, *20* (19), 3728−3733.
(8) Gould, T. E.; Piland, S. G.; Shin, J.; Hoyle, C. E.; Nazarenko, S. Characterization of Mouthguard Materials: Physical and Mechanical Properties of Commercialized Products. *Dent. Mater.* **2009**, *25* (6), 771−780.
(9) Gould, T. E.; Piland, S. G.; Shin, J.; McNair, O.; Hoyle, C. E.; Nazarenko, S. Characterization of Mouthguard Materials: Thermal Properties of Commercialized Products. *Dent. Mater.* **2009**, *25* (12), 1593−1602.
(10) Clark, T. S.; Hoyle, C. E.; Nazarenko, S. Kinetics Analysis and Physical Properties of Photocured Silicate-Based Thiol-ene Nanocomposites: The Effects of Vinyl POSS ene on the Polymerization Kinetics and Physical Properties of Thiol-triallyl Ether Networks. *J. Coat. Technol.* **2008**, *5* (3), 345−351.
(11) Phillips, J. P.; Mackey, N. M.; Confait, B. S.; Heaps, D. T.; Deng, X.; Todd, M. L.; Stevenson, S.; Zhou, H.; Hoyle, C. E. Dispersion of Gold Nanoparticles in UV-Cured, Thiol-ene Films by Precomplexation of Gold-Thiol. *Chem. Mater.* **2008**, *20* (16), 5240−5245.
(12) Owusu-Adom, K.; Schall, J.; Guymon, C. A. Photopolymerization Behavior of Thiol-acrylate Monomers in Clay Nanocomposites. *Macromolecules* **2009**, *42* (9), 3275−3284.
(13) Cramer, N. B.; Couch, C. L.; Schreck, K. M.; Boulden, J. E.; Wydra, R.; Stansbury, J. W.; Bowman, C. N. Properties of Methacrylate-thiol-ene Formulations As Dental Restorative Materials. *Dent. Mater.* **2010**, *26* (8), 799−806.
(14) Cramer, N. B.; Couch, C. L.; Schreck, K. M.; Carioscia, J. A.; Boulden, J. E.; Stansbury, J. W.; Bowman, C. N. Investigation of Thiol-ene and Thiol-ene-methacrylate Based Resins As Dental Restorative Materials. *Dent. Mater.* **2010**, *26* (1), 21−28.
(15) McNair, O. D.; Gould, T. E.; Piland, S. G.; Savin, D. A. Characterization of Mouthguard Materials: A Comparison of a Commercial Material to a Novel Thiolene Family *J. Appl. Polym. Sci.* **2014**, ASAP (10.1002/app.40402).
(16) Hoyle, C. E.; Lee, T. Y.; Roper, T. Thiol-enes: Chemistry of the Past with Promise for the Future. *J. Polym. Sci., Part. A: Polym. Chem.* **2004**, *42* (21), 5301−5338.
(17) Cramer, N. B.; Reddy, S. K.; Cole, M.; Hoyle, C.; Bowman, C. N. Initiation and Kinetics of Thiol-ene Photopolymerizations without Photoinitiators. *J. Polym. Sci., Part. A: Polym. Chem.* **2004**, *42* (22), 5817−5826.
(18) Chiou, B. S.; Khan, S. A. Real-Time FTIR and in Situ Rheological Studies on the UV Curing Kinetics of Thiol-ene Polymers. *Macromolecules* **1997**, *30* (23), 7322−7328.
(19) Hoyle, C. E.; Hensel, R. D.; Grubb, M. B. Laser-Initiated Polymerization of a Thiol-ene System. *Polym. Photochem.* **1984**, *4* (1), 69−80.
(20) Hoyle, C. E.; Lowe, A. B.; Bowman, C. N. Thiol-Click Chemistry: A Multifaceted Toolbox for Small Molecule and Polymer Synthesis. *Chem. Soc. Rev.* **2010**, *39* (4), 1355−1387.
(21) Li, Q.; Zhou, H.; Hoyle, C. E. The Effect of Thiol and Ene Structures on Thiol-ene Networks: Photopolymerization, Physical, Mechanical, and Optical Properties. *Polymer* **2009**, *50* (10), 2237−2245.
(22) Kolb, H. C.; Finn, M. G.; Sharpless, K. B. Click Chemistry: Diverse Chemical Function from a Few Good Reactions. *Angew. Chem., Int. Ed.* **2001**, *40* (11), 2004−2021.
(23) Service, R. F. Chemistry: Click Chemistry Clicks along. *Science* **2008**, *320* (5878), 868−869.
(24) Cramer, N. B.; Bowman, C. N. Kinetics of Thiol-ene and Thiol-acrylate Photopolymerizations with Real-Time Fourier Transform Infrared. *J. Polym. Sci., Part. A: Polym. Chem.* **2001**, *39* (19), 3311−3319.
(25) Senyurt, A. F.; Hoyle, C. E.; Wei, H.; Piland, S. G.; Gould, T. E. Thermal and Mechanical Properties of Cross-Linked Photopolymers Based on Multifunctional Thiol-urethane Ene Monomers. *Macromolecules* **2007**, *40* (9), 3174−3182.
(26) Yang, Z.; Wicks, D. A.; Hoyle, C. E.; Pu, H.; Yuan, J.; Wan, D.; Liu, Y. Newly UV-Curable Polyurethane Coatings Prepared by Multifunctional Thiol- and Ene-Terminated Polyurethane Aqueous Dispersions Mixtures: Preparation and Characterization. *Polymer* **2009**, *50* (7), 1717−1722.
(27) Shin, J.; Matsushima, H.; Chan, J. W.; Hoyle, C. E. Segmented Polythiourethane Elastomers through Sequential Thiol-ene and Thiol-isocyanate Reactions. *Macromolecules* **2009**, *42* (9), 3294−3301.
(28) Shin, J.; Matsushima, H.; Comer, C. M.; Bowman, C. N.; Hoyle, C. E. Thiol-isocyanate-ene Ternary Networks by Sequential and Simultaneous Thiol Click Reactions. *Chem. Mater.* **2010**, *22* (8), 2616−2625.
(29) Li, Q.; Zhou, H.; Wicks, D. A.; Hoyle, C. E. Thiourethane-Based Thiol-ene High Tg Networks: Preparation, Thermal, Mechanical, and Physical Properties. *J. Polym. Sci., Part. A: Polym. Chem.* **2007**, *45* (22), 5103−5111.
(30) Senyurt, A. F.; Wei, H.; Phillips, B.; Cole, M.; Nazarenko, S.; Hoyle, C. E.; Piland, S. G.; Gould, T. E. Physical and Mechanical Properties of Photopolymerized Thiol-ene/Acrylates. *Macromolecules* **2006**, *39* (19), 6315−6317.
(31) Lee, T. Y.; Carioscia, J.; Smith, Z.; Bowman, C. N. Thiol-allyl Ether-methacrylate Ternary Systems. Evolution Mechanism of Polymerization-Induced Shrinkage Stress and Mechanical Properties. *Macromolecules* **2007**, *40* (5), 1473−1479.
(32) Jian, Y.; He, Y.; Sun, Y.; Yang, H.; Yang, W.; Nie, J. Thiol-epoxy/Thiol-acrylate Hybrid Materials Synthesized by Photopolymerization. *J. Mater. Chem. C* **2013**, *1* (29), 4481−4489.
(33) McNair, O. D.; Sparks, B. J.; Janisse, A. P.; Brent, D. P.; Patton, D. L.; Savin, D. A. Highly Tunable Thiol-ene Networks via Dual Thiol Addition. *Macromolecules* **2013**, *46* (14), 5614−5621.
(34) Peeterbroeck, S.; Alexandre, M.; Jérôme, R.; Dubois, P. Poly(ethylene-co-vinyl acetate)/Clay Nanocomposites: Effect of Clay Nature and Organic Modifiers on Morphology, Mechanical, and Thermal Properties. *Polym. Degrad. Stab.* **2005**, *90* (2), 288−294.
(35) McNair, O. D.; Janisse, A. P.; Krzeminski, D. E.; Brent, D. E.; Gould, T. E.; Rawlins, J. W.; Savin, D. A. Impact Properties of Thiol-ene Networks. *ACS Appl. Mater. Interfaces* **2013**, *5* (21), 11004−11013.